Received: 26 July 2022 | Accepted: 12 September 2022

DOI: 10.1111/1751-7915.14151

RESEARCH ARTICLE

microbial biotechnology Open Access

The protein scaffold calibrates metal specificity and activation in MerR sensors

Julián I. Mendoza[1] | **Julián Lescano**[1] | **Fernando C. Soncini**[1,2] | **Susana K. Checa**[1,2]

[1]Instituto de Biología Molecular y Celular de Rosario (IBR), Universidad Nacional de Rosario (UNR)-Consejo Nacional de Investigaciones Científicas y Técnicas (CONICET), Rosario, Argentina

[2]Departamento de Microbiología, Facultad de Ciencias Bioquímicas y Farmacéuticas, Universidad Nacional de Rosario, Rosario, Argentina

Correspondence
Susana K. Checa, IBR (UNR-CONICET), Ocampo y Esmeralda, S2000EZP Rosario, Argentina.
Email: checa@ibr-conicet.gov.ar

Funding information
Agencia Nacional de Promoción de la Investigación, el Desarrollo Tecnológico y la Innovación, Grant/Award Number: PICT-2019-00333

Abstract

MerR metalloregulators are the central components of many biosensor platforms designed to report metal contamination. However, most MerR proteins are non-specific. This makes it difficult to apply these biosensors in the analysis of real environmental samples. On-demand implementation of molecular engineering to modify the MerR metal preferences is innovative, although it does not always yield the expected results. As the metal binding loop region (MBL) of these sensors has been proposed to be the major modulator of their specificity, we surgically switched this region for that of well-characterized specific and non-specific homologues. We found that identical modifications in different MerR proteins result in synthetic sensors displaying particular metal-detection patterns that cannot be predicted from the nature of the assembled modules. For instance, the MBL from a native Hg(II) sensor provided non-specificity or specificity toward Hg(II) or Cd(II) depending on the MerR scaffold into which it was integrated. These and other evidences reveal that residues outside the MBL are required to modulate ion recognition and transduce the input signal to the target promoter. Revealing their identity and their interactions with other residues is a critical step toward the design of more efficient biosensor devices for environmental metal monitoring.

INTRODUCTION

Heavy metals are persistent pollutants causing harsh environmental damages as well as diseases in humans and animals (Kumar et al., 2019; Sheldon & Skaar, 2019). Although some are essential for macromolecular structure and metabolism (e.g. zinc and copper), overdoses intoxicate cells as occurs with toxic metal ions like mercury, lead and cadmium that because of their physicochemical properties can affect cellular metabolic processes at very low concentrations (Checa et al., 2021; Jordan et al., 2020; Pontel et al., 2015). Bacterial resistance to these elements depends on a set of sensory proteins such as those of the MerR family of cytoplasmic regulators (Capdevila et al., 2017). This particular group of dimeric transcription factors have a common mechanism of gene modulation. Metal detection at the dimer interface is allosterically transduced through a currently unknown set of interactions to the DNA-binding domains leading to the transcriptional activation of genes required to overcome toxicity (Chang et al., 2015; Fang et al., 2021; Huang et al., 2016; Liu

et al., 2019; Philips et al., 2015; Wang et al., 2016). These bifunctional sensor/regulator proteins and their target promoters have been used for the construction of whole-cell biosensors (WCB), that is, genetically engineered microorganisms that couple metal detection to the production of an easily quantified output signal (Bereza-Malcolm et al., 2015; Checa et al., 2012; Kim et al., 2018; Saltepe et al., 2018). Unfortunately, most MerR sensors have low inducer-specificity and are activated by a group of cognate metal ions. In addition, most biosensor platforms display low dynamic range, that is, the ratio between the highest and the lowest output signals detected. These issues have hindered the application of these devices in the analysis of real contaminated samples (Roggo & van der Meer, 2017).

Specificity in metal detection by MerR sensors, which is the ability to discriminate one metal ion from others, is mainly determined by the protein scaffold and its ability to interact with the ion and drive the allosteric changes needed to modulate transcription of its target genes (Guerra & Giedroc, 2012). Metal binding at the protected dimer interface depends on the availability of ligands; in other words, the thiol group of conserved cysteine (Cys) residues in a proper array according to the coordination geometry preferred by each metal (Chang et al., 2015; Huang et al., 2016; Liu et al., 2019; Martell et al., 2015; Philips et al., 2015; Reyes-Caballero et al., 2011; Wang et al., 2016). Other residues from the metal-binding environment were proposed to tune this interaction by favouring recognition of one or a few cognate ions while excluding others (Cerminati et al., 2015; Ibáñez et al., 2013, 2015; Jia et al., 2020; Kang et al., 2018; Mendoza et al., 2020). For instance, the Cu sensor CueR binds Cu(I), but also Ag(I) or Au(I) in a linear two-coordinate geometry using the S-atoms of C112 and C120 from the same monomer (Changela et al., 2003; Checa et al., 2007; Chen et al., 2003; Ibáñez et al., 2013; Sameach et al., 2019; Szunyogh et al., 2015). These highly conserved Cys residues define the metal-binding loop (MBL) of 7 amino acids that in the Au-specific CueR paralogue, GolS, discriminates Au(I) from its cognates ions, Cu(I) and Ag(I) (Ibáñez et al., 2013) (Figure 1). In fact, CueR can be converted in an Au(I)-specific sensor just by switching its MBL by that of GolS, and contrariwise, GolS selectivity can be reversed by performing the converse replacement (Cerminati et al., 2015; Ibáñez et al., 2013).

In the group of MerR sensors responding to +2 metal ions, the contribution of the MBL region to tune metal specificity is not that clear. Typically, these sensors have a longer MBL compared with CueR-like proteins (Figure 1). Hg(II) coordination in the prototypical MerR sensor from the *Pseudomonas aeruginosa* Tn501 element (MerR-Tn) involves the Cys residues defining its MBL of one monomer and a third thiol ligand from another Cys residue in the other monomer (Wang et al., 2016, Figure 1). Its *Bacillus megaterium* MerR paralogue (MerR-Bm) binds Hg(II) using a similar trigonal planar geometry (Chang et al., 2015). Other +2 metal ion binding MerR homologues, such as PbrR or CadR, use either a trigonal-pyramidal stereoscopic array of thiol ligands or a tetrahedral geometry involving also a non-conserved asparagine residue to favour recognition of Hg(II), Pb(II) or Cd(II), respectively (Hobman et al., 2012; Huang et al., 2016; Wang et al., 2016). Thus, it seems that the 8-residue-long MBL of these sensors, with clearly different amino acid sequences, has a key role in determining this metal preferences. The Zn(II)/Pb(II)/Cd(II)-responding ZntR homologue conserves the three thiol ligands, but has a still longer MBL of 9 residues (Figure 1). This region includes additional Cys and histidine (His) residues that with the conserved cysteines are required to coordinate two Zn(II) atoms at the metal-binding site in the optimal tetrahedral array preferred by this ion (Changela et al., 2003; Khan et al., 2002). These additional MBL ligands are not required for the detection of Cd(II) or Pb(II) ions (Khan et al., 2002), although the coordination geometry adopted by these ions in the ZntR environment is unknown.

To explore the tunability in metal preference of MerR sensors, we previously added the third Cys residue to either CueR or GolS, mirroring to metal binding environment of the +2 metal ion sensors (Ibáñez et al., 2015). This modification resulted in non-specific sensors (named here CueR77 and GolS77, respectively, for simplicity) that respond to their native +1 inducers as well as to Hg(II) and to other +2 ions if the metal homeostasis of the bacterial chassis was artificially altered (Cerminati et al., 2015; Ibáñez et al., 2015). As the MBL is established as the main determinant of GolS Au-specificity, we also switched the GolS77-MBL for that of CueR to add Cu(I) and Ag(I) to the spectrum of metal detected by the synthetic sensor, and designed a set of WCB for rapid evaluation of water contamination (Cerminati et al., 2015). Accordingly, replacement of the GolS77-MBL for the equivalent region of MerR-Tn sensor switched sensor preferences to Hg(II) (Mendoza et al., 2020). The integration of this synthetic protein (named GolS77-LRT) into the GolS-dependent biosensor platform resident in an otherwise wild-type bacterial chassis resulted in a WCB that specifically reported bioavailable Hg(II) even in the presence of other toxic metals (Mendoza et al., 2020). Surprisingly, the analogous GolS77-LRB protein, containing the MBL of the Hg(II)-specific MerR-Bm sensor, responded to Au(I) as well as to Hg(II) under similar conditions, resembling the parental GolS77 protein (Mendoza et al., 2020). These results suggest that these MBL regions are not the only determinant of metal specificity in their native MerR sensors and in the GolS77 scaffold. In this study, we evaluated this point by replicating the -LRT and -LRB modifications in the paralogue CueR77 sensor, and tested the response metals of the analogous

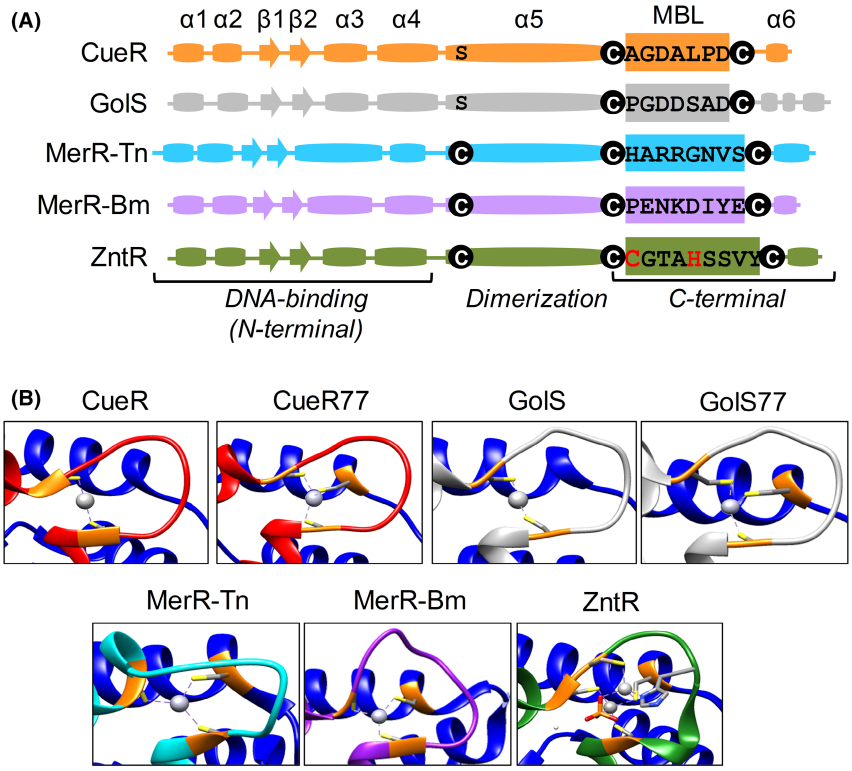

FIGURE 1 Structural features of the MerR sensors relevant for this study. (A) Schematic representation showing the array of α helices and β sheets, and the different parts conforming each monomer in CueR, GolS, MerR from the *P. aeruginosa* Tn501 element (MerR-Tn), MerR from *B. megaterium* (MerR-Bm) or ZntR. The conserved cysteines appeared inside black globes while other important residues are highlighted. The amino acid sequence composing the MBL region are depicted in full. (B) In silico models of the metal binding environment of the sensors showed in part A, and the CueR77 and GolS77 non-specific sensors. The PBD data bank codes for the sensor/metal complexes are: 1Q05, 5CRL, 4UA1 and 1Q08 for CueR/Cu(I), MerR-Tn/Hg(II), MerR-Bm/Hg(II) and ZntR/Zn(II), respectively. The SWISS-MODEL webserver and the CueR-Cu(I) crystals were used to modulate CueR77, GolS and GolS77. In each figure, the proximal monomer of the sensor is highlighted in the same colour used in part A, while the distal monomer is always coloured in blue. The cysteine/histidine residues that interact with the metal ion are highlighted in orange and their lateral chains depicted

CueR77- and GolS77-derivatives in a bacterial chassis with its +2 ion homeostasis artificially altered. We also tested other MBL modifications in these proteins as well as in the native Zn(II)/Pb(II)/Cd(II) sensor, ZntR, to obtain other MerR-like proteins with new metal-detection capacities. Our results suggest that, independently of the availability of metal ligands or the identity of residues within the MBL, the protein scaffold highly influences the metal sensing capacity of these biological sensors.

EXPERIMENTAL PROCEDURES

Strains, plasmids and cultured conditions

Salmonella enterica serovar Typhimurium (*S.* Typhimurium) strains and plasmids constructed or used in this study are listed in Tables S2 and S3, respectively. Except PB4406 and PB5295, all *S.* Typhimurium strains are derived from ATCC 14028s. *E. coli* DH5α was used for protein expression and purification. Bacteria were routinary grown at 37°C in Luria Broth (LB; Difco) or on LB-agar plates supplemented with 10 μg/ml chloramphenicol (Cm), 15 μg/ml tetracycline (Tc), 25 μg/ml kanamycin (Km) and/or 100 μg/ml ampicillin (Amp) as indicated in each case. Bacterial stocks (overnight cultures supplemented with 15% glycerol) were stored at −80°C until used. Reagents and chemicals were purchased from Merck and affiliates.

Genetic manipulations and plasmid constructions

Salmonella Typhimurium strains encoding the synthetic CueR77, GolS77 or GolS derivatives were constructed basically as previously described (Ibáñez et al., 2013; Mendoza et al., 2020). Briefly, we applied a two-step PCR protocol following by an overlap extension reaction using the Q5® High-Fidelity DNA Polymerase (New England Biolabs). This strategy is summarized in Figure S8. According to the synthetic protein to be constructed, we used total DNA from 14028s, PB12947 or PB9295 as templates (Table S2) and the oligonucleotides listed and described in Table S4. Each product

containing the synthetic sensor gene linked to the Cm^R cassette was independently introduced by electroporation into PB4406/pKD46 or PB5295/pKD46 strains (Tables S2 and S3) expressing the Lambda Red recombination system that catalyses sequence-specific chromosomal integration. After selection of Cm-resistant colonies, each synthetic sensor-Cm^R array was moved to the chromosome of the 14028s or its Δ*zntA* derivative (Table S2) by P22-mediated transduction. This technique was also used to move the *zntA*::*lacZY*$^+$ reporter construction to the Δ*zntR* strain chromosome to generate PB13171.

To obtain the expression plasmids pPB1491 and pPB1492, the genes encoding $golS77_{LRT}$ or $cueR77_{LRB}$ were PCR amplified from PB13416 or PB13691 chromosomes using either the golS-ORF-F/ golS-ORF-R or the cueR-ORF-F/cueR-ORF-R primer pair, respectively, and the Q5® enzyme (Table S4). The PCR products were treated with BamHI and HindIII, and cloned into pUH21-2 $laqI^q$ (Table S3) digested with the same enzymes. A similar strategy was used to amplify the *zntR* allele from the chromosomal DNA of 14028 s, and to introduce the desired modifications at its 3′ end. For this purpose, the ZntR-F primer was combined with each of the reverse primers carrying the MBL-coding sequence to be introduced (Table S4).

All chromosomal modifications or plasmid constructs were verified by DNA sequencing at Macrogen Inc., South Korea.

Metal induction determinations and western blot

0.5 or 1 M stock solutions of $HAuCl_4$, $CuSO_4$, $HgCl_2$, $CdCl_2$, $Pb(NO_3)_2$ or $ZnCl_2$ (ACS analytical grade ≥ 98.0% purity) were prepared using sterile ultrapure Milli-Q water and preserved at 4°C until used. Fresh working dilutions were daily prepared to apply a 10 μl aliquot onto each test tube. To avoid Pb^{2+} precipitation, cells were grown in minimal SM9 (M9 without NaCl) medium supplemented with 0.2% glucose and the required antibiotics. When necessary, isopropyl β-D-1-thiogalactopyranoside (IPTG) was added. Cells were grown at 37 °C with vigorous shaking until ~0.5 O.D. at 600 nm (OD600). At this point, the cultures were aliquoted in tubes containing each metal salt at the indicated final concentration. Incubation was allowed to continue for 3 more hours under identical conditions prior to determine the final OD600 and to perform the β-galactosidase activity essays on whole-cell extracts as previously described (Pérez Audero et al., 2010). The calculated β-galactosidase activity normalized against the final OD600 was expressed as Miller Units. When indicated, the induction coefficient was calculated as the ratio between the β-galactosidase values obtained from cells incubated in the presence and absence of metal ions.

To evidence metal-driving self-induction of the synthetic GolS variants as well as the accumulation of plasmid encoded synthetic GolS- or CueR-derived sensors, the whole-cell extracts obtained from overnight cultures were subjected to SDS-PAGE/western-blot analysis. Immunodetection was done using either anti-GolS or anti-CueR rabbit polyclonal antibodies and the SuperSignal West Femto Trial Kit (Thermo Scientific) essentially as described (Checa et al., 2007). Protein load was adjusted to 40 μg using the Bradford assay and bovine serum albumin as standard.

Protein purification and Cu-binding assay

CueR77 and CueR77-LRB were expressed and purified from *E. coli* DH5α/pPB1362 or DH5α/pPB1492, respectively, essentially as described previously (Espariz et al., 2007). Briefly, 0.5 mM IPTG was added to mid-exponential aerobically cultured cells to induce protein expression, and incubation was allowed to proceed for additional 4 h. Collected cells were disrupted by sonication and soluble proteins were precipitated with 45% $(NH_4)_2SO_4$, prior to affinity purification (HiTrap™ HP Heparin column; GE Healthcare) and gel filtration (Superdex 75 GL column; GE Healthcare). Protein concentration was determined by Bradford assay, using BSA as standard.

Copper-binding affinity assays were done basically as described (Quintana et al., 2017) by following the dissociation of the chromatophoric bathocuproinedisulfonic-Cu^+ ($CuBCS_2$) complex at 483 nM after 5 min competition with 1–20 μM CueR or CueR-LRB at room temperature. Protein-Cu^+ dissociation constant (K_D) values were calculated by fitting the experimental data to the following equilibrium equation.

$$\frac{[\text{protein}]_t}{[Cu^+]_t} = 1 - \frac{[CuBCS_2]}{[Cu^+]_t} + K_D\beta_2\left(\frac{[BCS]_t}{[CuBCS_2]} - 2\right)^2 [CuBCS_2]\left(1 - \frac{[CuBCS_2]}{[Cu^+]_t}\right)$$

where *t* is total and β_2, the formation constant reported for $CuBCS_2$ equal to $10^{19.8}$ M^{-2}, ε = 13,000 M^{-1} cm^{-1} (Xiao et al., 2011).

In silico modelling and analysis

Each of the tested synthetic sensors were in silico modelling using SWISS-MODEL (https://swissmodel.expasy.org; Waterhouse et al., 2018) and the crystallographic structures of CueR-Cu(I) (1Q05) or ZntR-Zn(II) (1Q08). The Chimera program (Pettersen et al., 2004) were employed to visualize and compare the structures of these synthetic proteins and their native sensors.

Incorrect metal assignments or geometrical irregularities at the metal-binding site of CueR and ZntR derivatives were predicted using the Checkmymetal (CMM) server (https://cmm.minorlab.org) and the native proteins as templates. This program (Zheng et al., 2017) evaluates the atomic composition of the first metal coordination sphere, predicts the potential metal ligands and calculates different parameters that are detailed as notes in Table S1.

RESULTS

MBLs from Hg-sensors decrease CueR77 response to +1 ions but do not improve Hg(II) selectivity

The MBL region from the MerR-Tn Hg(II) sensor, LRT, confers Hg(II) specificity to GolS77 by decreasing responsiveness to Au(I), the native GolS inducer (Mendoza et al., 2020). Because GolS and CueR are close paralogues, it is expected that replacing the native CueR77-MBL for the 8-residue-long LRT region will render a Hg(II)-specific CueR derivative. The *cueR77*$_{LRT}$ gene was generated and inserted into the *Salmonella enterica* serov. Typhimurium (*S.* Typhimurium) chromosome, replacing the *cueR* gene. (Note that according to our prior results (Cerminati et al., 2011, Ibáñez et al., 2013, 2015, Pérez Audero et al., 2010], expression of CueR-like sensors from the chromosome improves metal response and selectivity.) In addition, the gene coding for the ZntA transporter was deleted from the chromosome of the transgenic *S.* Typhimurium *cueR77*$_{LRT}$ strain in order to increase the intracellular availability of Zn(II), Cd(II) and Pb(II), which are known inducers of the parental CueR77 sensor in these conditions (Ibáñez et al., 2015). Finally, the cells were transformed with pP*copA-lacZ*, a plasmid harbouring the CueR-dependent P*copA* promoter controlling the expression of the *lacZ* reporter gene (see Experimental Procedures for details). The biosensing capacity of the synthetic CueR77-LRT sensor was evaluated by determining β-galactosidase activity on whole-cell extracts from cultures exposed for 3 h to Cu, Au, Hg, Pb or Cd salts (Figure 2). Δ*zntA* strains expressing CueR77, GolS77-LRT or GolS77, and carrying proper reporter plasmids, were included as controls.

Contrary to our predictions, the LRT region did not increase Hg(II) selectivity in the CueR77 scaffold (Figure 2A). In fact, CueR77-LRT exhibited a decreased response to Hg(II), Au(I) or Zn(II) compared with the parental CueR77, but similar Cd(II)- or Pb(II)-directed induction of the reporter. Remarkably, the CueR77-LRT-based biosensor could not report Cu(I) (Figure 2A), the physiologically relevant CueR and CueR77 inducer (Pontel et al., 2015). In the Δ*zntA* strain, the Hg(II) preference of GolS77-LRT previously

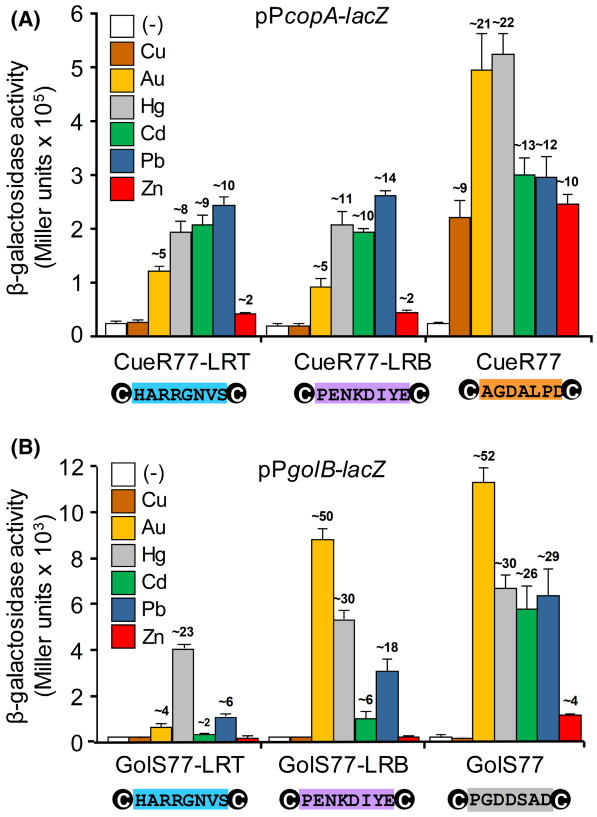

FIGURE 2 Identical MBL modifications on CueR77 and GolS77 provide different metal detection patterns. β-galactosidase activity determinations were done on whole cell extracts obtained from reporter Δ*zntA* strains expressing the indicated CueR77 (A) or GolS77 (B) derivative. pP*copA-lacZ* or pP*golB-lacZ* are the CueR- or GolS-dependent reporter plasmids. Mid-exponential cell cultures were incubated in minimal SM9 medium at 37°C with shaking for 3 h with 10 μM $Cu(SO_4)$ (Cu), 10 μM $AuHCl_4$ (Au), 1 μM $HgCl_2$ (Hg), 1 μM $CdCl_2$ (Cd), 1 μM $Pb(NO_3)_2$ (Pb) or 100 μM $ZnCl_2$ (Zn). (–) means no metal addition. Activity is expressed as Miller units. Significant induction levels (in n-fold) relative to uninduced samples (–) are indicated at the top of each bar. The data represent the mean ± *SD* of six independent measurements done in duplicate

noticed in the wild-type chassis (Mendoza et al., 2020) is preserved, and its pattern of metal-directed activation certainly differed from that of the non-specific CueR77-LRT sensor (Figure 2).

In view of these results, we introduced the LRB region derived from the MerR-Bm Hg(II) sensor into CueR77. This MBL has the same length (eight residues) but different amino acid sequence than the LRT region (see Figure 1A). As mentioned in the introduction, in the GolS77 scaffold this modification resulted in a non-selective Au/Hg sensor when assayed in an otherwise wild-type bacterial chassis (Mendoza et al., 2020). In the Δ*zntA* environment tested here, the synthetic CueR77-LRB sensor exhibited a similar pattern of metal activation than CueR77-LRT, including the lack of response to Cu(I). Dose–response curves for all CueR77 derivatives not only confirmed these results, but also allowed us to verify the decreased response of both CueR77-LRT and CueR77-LRB to Au(I), Hg(II) or Zn(II), as well as their

unresponsiveness to Cu ions (Figure S1). As LRT, introduction of the LRB region in the scaffold of either CueR77 or GolS77 differently affected the metal-detection capacity of the resulting biosensors (Figure 2). In the Δ*zntA* reporter strain, GolS77-LRB exhibited a singular metal induction pattern that does not resemble that of GolS77-LRT or of any of the CueR77-derivatives assayed here. Compared to the parental GolS77 sensor, GolS77-LRB retained its response to both Au(I) and Hg(II), but it was less responsive to Pb(II) or Cd(II) (Figure 2B). It was insensitive to Zn(II) as well. Similar results were obtained by (i) testing the accumulation of the self-inducted chromosomally encoded GolS77 derivatives (Figure S2) or (ii) expressing CueR-LRB or GolS-LRT from multicopy plasmids and measuring the transcriptional activity derived from chromosomally encoded CueR/GolS-dependent reporters (Figure S3).

The LRB modification in CueR77 decreases but does not impair Cu(I) binding

According to the current model, the ability of MerR sensors to differentiate an inducing ion from a non-inducing ion depends not only on metal binding, but also on how the input signal is transduced to the target promoter through the protein scaffolding (Fang et al., 2021; Martell et al., 2015; Philips et al., 2015; Sameach et al., 2019). Thus, the lack of response to Cu(I) of CueR77-LRT and CueR77-LRB might result from either improper Cu(I) binding and/or from defective transduction of the input signal to the DNA binding-domain. An in silico simulation of the Cu(I) coordination environment in these synthetic CueR proteins using the CMM web tool (https://cmm.minorlab.org) revealed that the metal ion is bound by three thiol ligands (possible C77, C112, and C120) in a trigonal planar geometry, as occurs in CueR77 (Table S1). However, the calculated nVECSUM values for CueR77-LRT and CueR77-LRB increased at least 3-fold compared to the parental sensor. This suggests a marked asymmetry in the coordination environment that would disfavour their interaction with Cu(I). (Note that 0.1 is the threshold nVECSUM value proposed as acceptable in metal-ligands geometric arrangement (Zheng et al., 2017)). As expected, the native Cu(I) sensor CueR, included in the analysis as a control, exhibited a lineal di-coordination geometry to the S-groups of C112 and C120 as reported (Changela et al., 2003) and the minimal nVECSUM value among the analysed sensors.

To evaluate the in vitro interaction with Cu(I), CueR77-LRB and CueR77 were purified and their abilities to extract the metal ion from the chromophoric $CuBCS_2$ complex were analysed (see Experimental Procedures for details). As shown in Figure 3, the LRB modification in CueR77 significantly decreased, but not impaired Cu(I)-binding. The dissociation constant (K_D) calculated for CueR77-LRB was $6.99 \pm 0.61 \times 10^{-17}$ M, one order of magnitude lower than that of the parental sensor. However, this value is comparable to that of Cu chaperones, well-known Cu(I) cytoplasmic transporters (Quintana et al., 2017; Xiao et al., 2011). Based on these results and the lack of in vivo response to Cu(I) (Figure 2A and Figure S1), we predict that CueR77-LRB cannot drive the allosteric changes needed to activate transcription in the presence of Cu ions. Although certainly this hypothesis awaits elucidation, it is supported by recent reports showing that CueR interacts in vitro with either Hg(II) or Cd(II), but these metals cannot switch the sensor to its transcriptional active form (Balogh et al., 2019, 2020).

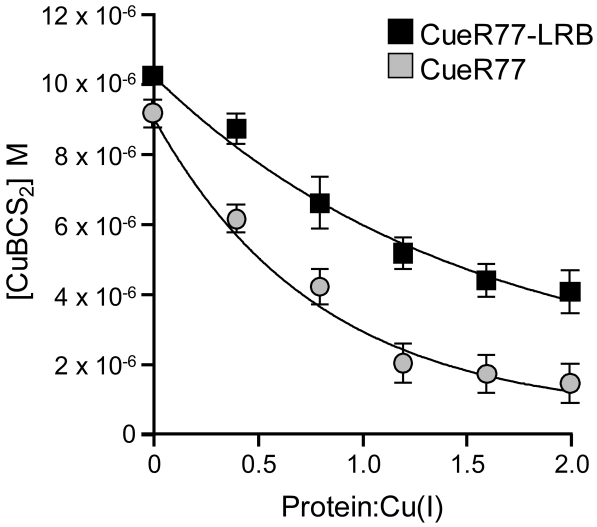

FIGURE 3 The CueR-LRB sensor binds Cu(I) ions. $CuBCS_2$/CueR77 and $CuBCS_2$/CueR77-LRB competition assays were done in triplicates. Reaction mixtures were prepared with constant concentrations of Cu^{2+} (10 μM) and BCS (25 μM) and varying concentrations of the purified CueR-like protein (1–20 μM monomer). The experimental data were fit to the equilibrium binding equation to calculate the dissociation constant (K_D) of each protein/Cu(I) complex. See the Materials and Methods section for details. The calculated K_D values were $6.6 \pm 0.51 \times 10^{-18}$ M and $6.99 \pm 0.61 \times 10^{-17}$ M for the CueR77/Cu(I) and CueR77-LRB/Cu(I) complexes, respectively

The MBL of ZntR has different effects on metal detection when is integrated into the CueR77 or the GolS77 scaffold

To determine if the scaffold-dependent effects on the metal-detection pattern of sensors having the -LRT and -LRB modifications is extensive to other MBL sequences, we replaced this region in both CueR77 and GolS77 for that of ZntR, the well-characterized Zn(II)/Pb(II)/Cd(II) sensor (Binet & Poole, 2000; Changela et al., 2003; Gireesh-Babu & Chaudhari, 2012). The ZntR-MBL sequence (named here LZ for simplicity) is one and two residues longer than the LRT/LRB regions or the native CueR/GolS MBLs, respectively (see Figure 1A). To

test the response to metals of the -LZ derivatives, the synthetic *cueR77*$_{LZ}$ and *golS77*$_{LZ}$ genes were generated and inserted in the chromosome of Δ*zntA* reporter strains as described above. As the LZ region includes the Cys and His residues, ZntR uses to coordinate two Zn(II) atoms in the optimal tetrahedral array (see Figure 1); we expected this MBL modification in either CueR77 or GolS77 will render better Zn(II)-detectors than the parental sensors. Contrary to our expectations, CueR77-LZ decreased more than 3-fold its response to Zn(II) ions compared to CueR77 (Figure 4A). Furthermore, this sensor exhibited a pattern of metal detection that resembles those of CueR77-LRT and CueR77-LRB (see Figure 2A). As the other CueR77 derivatives, the CueR77-LZ sensor resulted insensitive to Cu(I) in a broad range of concentrations, and responded poorly to the other metals, but particularly to Au(I) or Hg(II) (Figure S4). Accordingly, CMM simulation showed that Cu(I) binding is highly disfavoured in the CueR77-LZ environment with the higher nVECSUM value among the tested CueR derivatives (Table S1). This was accompanied by a change in the predicted coordination geometry to a tetrahedral array involving both S and N atoms, and a 25% vacancy on its binding sites.

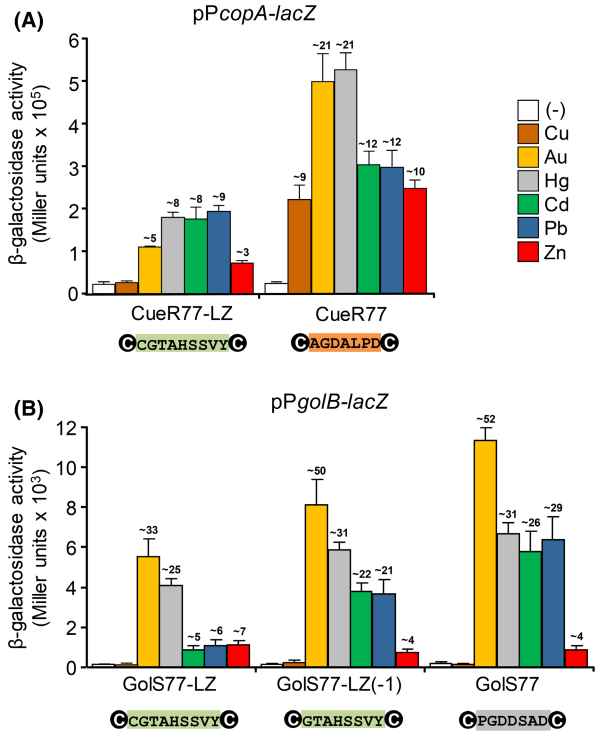

FIGURE 4 A similar scaffold-dependent effect on metal detection was observed after inserting the LZ sequence on CueR77 and GolS77. *Salmonella* Δ*zntA* reporter strain expressing the indicated CueR77 (A) or GolS77 (B) derivative were grown and used to perform β-galactosidase activity determinations as in Figure 2. The results were shown in Miller units. As in Figure 2, significant induction levels (in n-fold) were indicated above each bar. The reporter plasmid carrying by the cells are indicated in the upper part of each graphic. The data represent the mean ± *SD* of five independent measurements done in duplicate

On the other hand, the LZ replacement in GolS77 provided a metal-detection pattern that did not resemble CueR77-LZ (Figure 4) or the others GolS77 derivatives (see Figure 2B). As noticed, GolS77-LZ detected Au(I) or Hg(II) as GolS77-LRB, although with significant low efficiency, and contrary to this sensor, it poorly responded to both Cd(II) and Pb(II). These results were verified by testing the accumulation of the self-induced GolS77-LZ in whole cell extracts (see Figure S2). Interestingly, the LZ modification in the GolS77 scaffold increased the ability to perceive Zn(II), contrasting with CueR77-LZ in which this modification had negative effects on Zn(II) detection (Figure 4).

The diminished biosensing capacity of GolS77-LZ compared to the other GolS77 and CueR77 derivatives (compared Figures 4 and 2) could be caused by either the extension of the loop between the metal-coordinating C residues or the presence of three consecutive Cys residues (C111-C112-C113) that perhaps disturb metal interaction and/or affect the allosteric transduction of the signal to the target promoter (Guerra & Giedroc, 2012). The last array is not present in the CueR77-LZ paralogue which lacks the C111 residue. To test this, we generated the GolS77-LZ(–1) sensor, in which the additional MBL-located ligand, C113, was removed. This modification also provided a MBL of eight residues as LRT and LRB but with different amino acid sequence. As shown in Figure 4B, the LZ(–1) modification decreased the response to Zn(II) to the levels of the parental sensor while improved detection of Au(I), Hg(II), Pb(II) or Cd(II) comparing with GolS77-LZ. As the rest of the GolS/GolS77 derivatives ((Checa et al., 2007, Cerminati et al., 2011, 2015, Ibáñez et al., 2013, 2015, Mendoza et al., 2020), and Figure 2B), GolS77-LZ and GolS77-Z(–1) remained insensitive to Cu(I) (Figure 4B). We replicated the LZ and LZ(–1) modification in the native GolS sensor and observed similar results regarding Au(I)-directed activation of the reporter (Figure S5). That is, poor metal detection as the length of the MBL region in the sensor protein increased. This negative MBL-size/metal-response correlation was not noticed in the CueR77 derivatives (compared Figures 4A and 2A), and emerged as another evidence of the importance of the sensor scaffold on metal recognition.

The LRT region provides Cd(II) specificity to ZntR by decreasing its response to other +2 ions

As a model of sensors responding to +2 ions, we analysed the effects of switching the MBL region in the *S.* Typhimurium ZntR sensor that, like its *E. coli* paralogue (Binet & Poole, 2000), induced the expression of the ZntA transporter in response to Zn(II), Cd(II) or Pb(II) (Figure S6). This sensor slightly activated the expression of the *zntA-lacZ* reporter in the presence of Hg(II), but it

did not respond to Au or Cu ions, either when expressed form its chromosomal copy or from a plasmid (Figures S6 and 5). Thus, if the MBL is the main determinant of metal recognition, replacement of the 9-residue MBL of ZntR for that of GolS (named here LG for simplicity) (Figure S7A) would confer the ZntR-LG protein the ability to detect Au(I). In addition, this modification is predicted to disfavour Zn(II) interaction (see Table S1). Because *zntR* is the second gene of an operon, ant it is surrounded by genes of unknown function both in *S.* Typhimurium and *E. coli*, we cloned the synthetic $zntR_{LG}$ gene in a low copy-number plasmid under the control of the regulated *lac* promoter (see Experimental Procedures for details). The pPB1488 (pZntR-LG) plasmid was introduced into a Δ*zntR* strain carrying the P*zntA-lacZ* reporter replacing the chromosomal *zntA* copy. Reporter Δ*zntR* P*zntA-lacZ* strains carrying the pPB1486 (pZntR) or the plasmid vector were included in the assays either as a control or to normalized β-galactosidase activity determinations, respectively. Contrary to our expectations, the LG modification in ZntR did not stimulate Au(I)-detection (Figure 5). In fact, the synthetic ZntR-LG sensor resulted rather insensitive to most metal ions when expressed at low levels (Figure 5A), and a Cd(II)/Pb(II) detector when expression levels of the sensor increased as consequence of IPTG addition (Figure 5B).

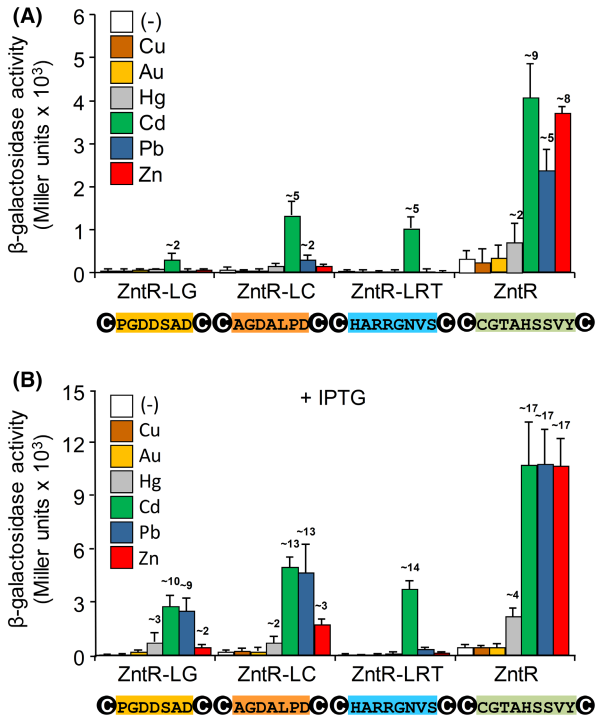

FIGURE 5 Modification of the MBL region of ZntR modifies the metal-detection pattern in a manner that cannot be predicted. *Salmonella* Δ*zntR* reporter strains expressing the native ZntR sensor or each of the indicated synthetic sensors from plasmids were grown without (A) or 100 μM of IPTG (B) in the presence of different metal salts (see Figure 2 for details). The reporter strain carrying the empty vector was also included in the assays as a control. β-galactosidase activity was determined in whole cell extracts as described in Figure 2. The calculated activity values (in Miller units) were normalized against the control sample (270 ± 28 Miller units). Significant induction levels (in n-fold) relative to uninduced samples (–) are indicated at the top of each bar. The data represent the mean ± *SD* of seven independent measurements done in duplicate

In view of these results, new synthetic ZntR-based sensors were constructed: ZntR-LC, which has the CueR-MBL (same size but different amino acid sequence than LG), and ZntR-LRT, which includes the eight residue-long region derived from the MerR-Tn Hg(II) sensor (Figure S7A). As ZntR-LG, none of these synthetic sensors acquired the metal-detection capacities of the MBL donor (i.e., the ability to respond either to Cu(I)/Au(I) or to Hg(II), respectively) even when IPTG was added to the cultures (Figure 5). This indicates that the MBL region per se does not determine metal preference in the ZntR scaffold. The modifications also disfavoured detection of the physiological ZntR inducer, Zn(II) (Figure 5), supporting the CMM predictions (Table S1). Interestingly, in the absence of IPTG, both ZntR-LC and ZntR-LRT induced 6-fold expression of the P*zntA*::*lacZ* reporter specifically in response to Cd(II) (Figure 5A). However, upon IPTG addition, only the ZntR-LRT sensor preserved specificity toward this metal ion (Figure 5B and Figure S7B). These results suggest that the LRT region alters the geometry of the coordination environment of ZntR to privilege productive Cd(II) recognition.

The Cd(II)-specific biosensing capacity of ZntR-LRT was tested in a broad range of $CdCl_2$ or $Pb(NO_3)_2$ concentrations (Figure S7C). This analytical tool reported bioavailable Cd in the 0.4–10 μM range (equivalent to 45–1123 μg/L), and allowed its quantification until 2.5 μM (280 μg/L), the concentration at which maximal induction of the P*zntA*::*lacZ* reporter (≥15-fold) is reached. Contrasting with the ZntR-LC and the parental ZntR, the ZntR-LRT is insensitive to Pb(II) ions at all concentrations tested (Figure S7C). These parameters support the biosensor qualities of this synthetic construction.

DISCUSSION

In the current era of synthetic biology, a common strategy to improve the performance of MerR-based WCBs is to rational engineering the metal-binding environment of the sensor protein to achieve specificity (Belkin & Wang, 2022; Galvão & de Lorenzo, 2006). Besides the number of thiol ligands required for metal-coordination, the MBL sequence was proposed to be the main determinant of specificity, at least in the group of MerR sensors responding to +1 ions. In this study, we applied rational MBL-switching protocol among different MerR-like sensors to develop new tools for metal detection and to explore the contribution of the MBL to metal specificity. Our results demonstrate that the foreign MBL does not determine the metal-detection pattern of the synthetic sensors. In fact, they suggest the requirement of other

regions of the protein scaffold to modulate metal recognition and/or to productively transduce the input signal to the target promoter to activate transcription.

CueR and GolS are structural and functional paralogues that only differ in their ability to discriminate Au(I) from other +1 cognate metal ions (Cerminati et al., 2011; Checa et al., 2007). This feature depends exclusively on the amino acid sequence of their MBL regions. In fact, Au(I)-specificity can be added or reversed between these paralogues just by exchanging their MBLs (Ibáñez et al., 2013). This MBL-determined metal preference is not even altered when the parental protein carried the S77C mutation that allow these biological sensors to recognized in addition +2 metal ions (Cerminati et al., 2015; Ibáñez et al., 2015). Thus, if this rule applies to the MerR group of +2 ion sensors as well, insertion of one of their MBL region into either CueR77 or GolS77 would similarly modify metal preferences, resembling those of the MBL-donor. Contrary to our expectations, the analogous CueR77- or GolS77-derivatives exhibited clearly different metal-detection pattern. This reveals a yet unappreciated role of scaffold proteins in modulating metal detection.

Irrespective of the MBL analysed, all CueR77 derivatives shared common characteristics: (i) significant reduction in their ability to respond to Au(I), Hg(II) or Zn(II) compared to the parental CueR77 sensor, but similar levels of Cd(II)- or Pb(II)-directed activation; and (ii) a remarkable insensitivity to Cu(I) (Figures 2, 4 and S1) more probably due to impaired allosteric transduction of the signal to the target promoter than to their lack of interaction with this metal ion (Figure 3). These results indicate that, in the CueR scaffold, the nature of the MBL region in terms of amino acid sequence, length or origin does not influence metal preference. This conclusion cannot be extended to the GolS77 derivatives, since identical MBL modifications in this protein scaffold resulted in synthetic sensors with particular metal-detection patterns and varying degrees of metal preferences that do not resemble any of the CueR77 derivatives nor their parental sensors. Even in cells with high intracellular levels of Zn(II), Pb(II) and Cd(II), only the introduction of the MBL of the MerR-Tn sensor into the GolS77 scaffold privileged Hg(II) recognition as in the original MBL-donor, while no such correlation was found in the rest of the GolS77 derivatives (Figures 2, 4 and S2). GolS77-LRB resulted in an efficient Au/Hg/Pb sensor, GoS77-LZ in a rather Au/Hg sensor and GolS77-LZ(–1) exhibited a metal induction profile that resembled the parental sensor. Consequently, in the GolS77 scaffold, it is not the MBL itself but its particular interaction with residues from other parts of the sensor which determines metal detection of the synthetic protein. Interestingly, all the GolS77 derivatives but also the GolS-LZ and GolS-LZ(–1) sensors retained the Cu(I) insensitivity of the parental sensor (Figures 2, 4, S2 and S5), a phenotype that only the MBL of CueR (LC) can revert (Cerminati et al., 2015; Checa et al., 2007; Ibáñez et al., 2013). These observations support the notion that besides the MBL length and sequence, other residues from the GolS scaffold were selected during evolution to privilege Au(I) recognition.

Another distinctive feature of all GolS77/GolS derivatives is the negative effect that the extension in the MBL region produced on the biosensing capacity, which even affect Au(I) detection (Figures 4 and S5). This suggests that, contrary to CueR, the GolS scaffold exhibited some molecular constrains to accommodate large MBL sequences at their metal-binding environment. Despite this, even the synthetic GolS-LZ and GolS77-LZ sensors having the largest MBL sequence are powerful bio detectors, as they activated reporter expression more than 25-fold in response to Au(I) or Au(I)/Hg(II), respectively (Figures 4 and S5). The remarkable biosensor capability of all GolS/GolS77-based platforms depends mostly on self-control of the regulator (Figure S2), a positive feedback loop that maximizes signal/noise ratio improving determinations (Cerminati et al., 2011, 2015; Mendoza et al., 2020).

Further confirmation to the hypothesis that the MBL region does not determine per se the metal detection pattern of MerR sensors was obtained from the application of the MBL-switching approach on the ZntR scaffold. Insertion of the MBL of either GolS or CueR in this protein did not privilege Au(I) or Cu(I)/Ag(I)/Au(I) detection, as expected (Figure 5). Furthermore, the LRT region that provides Hg(II) preference in the GolS77 scaffold (Figure 2), as in its innate MerR sensor, privileged Cd(II)-specific detection in the ZntR metal-binding environment (Figures 5 and S7). Thus, the response to metals of ZntR is also modulated by the interaction between the MBL and the rest of the sensor scaffold. As noticed, ZntR-LRT Cd(II) specificity is not the result of an enhanced recognition of this ion but of the lack of activation of the synthetic sensor by all the others ZntR inducers, including Hg(II). Other authors' reports support our observations. Replacements of ZntR or CadR MBLs for a set of synthetic, artificially designed peptide fragments switched metal preferences of the synthetic sensors to one of their native inducers, but with none or minimal increase in response to it compared with the parental sensors (Hyojin et al., 2020; Kang et al., 2018). Similar results were obtained after application of direct evolution approaches to modify metal-binding preferences MerR or PbrR (Hakkila et al., 2011; Jia et al., 2020). Interestingly, none of these modifications conducted to the acquisition of new biosensor capabilities as we achieved using the GolS scaffold (Cerminati et al., 2015; Mendoza et al., 2020). This suggested that MerR +2 ion sensors lacks the plasticity that this native Au(I) detector has. These results put the GolS scaffold as a good candidate for further synthetic manipulation and the obtention of a battery of improved WCB for metal monitoring.

Until now, the combined influence of many residues in determining metal selectivity of MerR sensors has been

suggested although not systematically proved. The data presented here indicate that, in most cases, the MBL region of the synthetic sensor cannot determines metal selectivity on its own. In fact, the metal preference is highly influenced by the rest of the sensor scaffold, probably by non-conserved residues that reside at the first or the second metal-coordination shell or connect these parallel metal-binding regions in the sensor dimer with the distal DNA-binding region. In the crystallographic structures of CueR and ZntR in complex with their inducer metals (Changela et al., 2003), the MBL of one monomer interacts with the N-terminal end of the dimerization α5 helix, as well as with the preceding α4-α5 loop of the other monomer (Figure 1). Also, the short C-terminal α6 helix following the MBL in CueR brings closer to the DNA-binding domain of the other monomer, both dimerization helices, and even contributes to charge neutralization of the -S group of C120 (Philips et al., 2015). Other transient interaction between residues that these structural studies could not reveal were proposed to modulated metal recognition and/or direct signal/transduction against the dimer interface (Fang et al., 2021; Martell et al., 2015; Sameach et al., 2019). Probably, these interactions have also had a crucial role in the evolution of this broad family of biological metal sensors. Revealing these interactions will contribute not only to explaining the differential effects on metal specificity resulting from the integration of the LRT region into the GolS77 and ZntR scaffolds reported here, but also to developing new synthetic tools for improving molecular engineering of MerR sensors on demand.

ACKNOWLEDGEMENTS

J.M. and J.L. are fellows of CONICET. S.K.C. and F.C.S. are career investigators of CONICET and Professors of the UNR. F.C.S. is also a career investigator of the Rosario National University Research Council (CIUNR). This work was supported by Grants from the Agencia Nacional de Promoción de la Investigación, el Desarrollo Tecnológico y la Innovación (Agencia I+D+I) of Argentina (PICT-2019-00333) to S.K.C.

FUNDING INFORMATION

Grant from the Agencia Nacional de Promoción de la Investigación, el Desarrollo Tecnológico y la Innovación (Agencia I+D+I) of Argentina (PICT-2019-00333) to S.K.C.

CONFLICT OF INTEREST

The authors have no conflicts to declare.

ORCID

Julián I. Mendoza https://orcid.org/0000-0002-1975-3606
Fernando C. Soncini https://orcid.org/0000-0002-8925-7763
Susana K. Checa https://orcid.org/0000-0003-1629-2848

REFERENCES

Balogh, R.K., Gyurcsik, B., Hunyadi-Gulyás, É., Schell, J., Thulstrup, P.W., Hemmingsen, L. et al. (2019) C-terminal cysteines of CueR act as auxiliary metal site ligands upon HgII binding—a mechanism to prevent transcriptional activation by divalent metal ions? *Chemistry – A European Journal*, 25, 15030–15035.

Balogh, R.K., Gyurcsik, B., Jensen, M., Thulstrup, P.W., Köster, U., Christensen, N.J. et al. (2020) Flexibility of the CueR metal site probed by instantaneous change of element and oxidation state from AgI to CdII. *Chemistry – A European Journal*, 26, 7451–7457.

Belkin, S. & Wang, B. (2022) Sense and sensibility: of synthetic biology and the redesign of bioreporter circuits. *Microbial Biotechnology*, 15, 103–106.

Bereza-Malcolm, L.T., Mann, G. & Franks, A.E. (2015) Environmental sensing of heavy metals through whole cell microbial biosensors: a synthetic biology approach. *ACS Synthetic Biology*, 4, 535–546.

Binet, M.R.B. & Poole, R.K. (2000) Cd(II), pb(II) and Zn(II) ions regulate expression of the metal-transporting P-type ATPase ZntA in *Escherichia coli*. *FEBS Letters*, 473, 67–70.

Capdevila, D.A., Edmonds, K.A. & Giedroc, D.P. (2017) Metallochaperones and metalloregulation in bacteria. *Essays in Biochemistry*, 61, 177–200.

Cerminati, S., Soncini, F.C. & Checa, S.K. (2011) Selective detection of gold using genetically engineered bacterial reporters. *Biotechnology and Bioengineering*, 108, 2553–2560.

Cerminati, S., Soncini, F.C. & Checa, S.K. (2015) A sensitive whole-cell biosensor for the simultaneous detection of a broad-spectrum of toxic heavy metal ions. *Chemical Communications*, 51, 5917–5920.

Chang, C.-C., Lin, L.-Y., Zou, X.-W., Huang, C.-C. & Chan, N.-L. (2015) Structural basis of the mercury(II)-mediated conformational switching of the dual-function transcriptional regulator MerR. *Nucleic Acids Research*, 43, 7612–7623.

Changela, A., Chen, K., Xue, Y., Holschen, J., Outten, C.E., O'Halloran, T.V. et al. (2003) Molecular basis of metal-ion selectivity and zeptomolar sensitivity by CueR. *Science*, 301, 1383–1387.

Checa, S.K., Espariz, M., Pérez Audero, M.E., Botta, P.E., Spinelli, S.V. & Soncini, F.C. (2007) Bacterial sensing of and resistance to gold salts. *Molecular Microbiology*, 63, 1307–1318.

Checa, S.K., Giri, G.F., Espariz, M., Argüello, J.M. & Soncini, F.C. (2021) Copper handling in the *Salmonella* cell envelope and its impact on virulence. *Trends in Microbiology*, 29, 384–387.

Checa, S.K., Zurbriggen, M.D. & Soncini, F.C. (2012) Bacterial signaling systems as platforms for rational design of new generations of biosensors. *Current Opinion in Biotechnology*, 23, 766–772.

Chen, K., Yuldasheva, S., Penner-Hahn, J.E. & O'Halloran, T.V. (2003) An atypical linear cu(I)–S2 center constitutes the high-affinity metal-sensing site in the CueR Metalloregulatory protein. *Journal of the American Chemical Society*, 125, 12088–12089.

Espariz, M., Checa, S.K., Pérez Audero, M.E., Pontel, L.B. & Soncini, F.C. (2007) Dissecting the *Salmonella* response to copper. *Microbiology*, 153, 2989–2997.

Fang, C., Philips, S.J., Wu, X., Chen, K., Shi, J., Shen, L. et al. (2021) CueR activates transcription through a DNA distortion mechanism. *Nature Chemical Biology*, 17, 57–64.

Galvão, T.C. & de Lorenzo, V. (2006) Transcriptional regulators à la carte: engineering new effector specificities in bacterial regulatory proteins. *Current Opinion in Biotechnology*, 17, 34–42.

Gireesh-Babu, P. & Chaudhari, A. (2012) Development of a broad-spectrum fluorescent heavy metal bacterial biosensor. *Molecular Biology Reports*, 39, 11225–11229.

Guerra, A.J. & Giedroc, D.P. (2012) Metal site occupancy and allosteric switching in bacterial metal sensor proteins. *Archives of Biochemistry and Biophysics*, 519, 210–222.

Hakkila, K.M., Nikander, P.A., Junttila, S.M., Lamminmaki, U.J. & Virta, M.P. (2011) Cd-specific mutants of mercury-sensing regulatory protein MerR, generated by directed evolution. *Applied and Environmental Microbiology*, 77, 6215–6224.

Hobman, J.L., Julian, D.J. & Brown, N.L. (2012) Cysteine coordination of pb(II) is involved in the PbrR-dependent activation of the lead-resistance promoter, PpbrA, from *Cupriavidus metallidurans* CH34. *BMC Microbiology*, 12, 109.

Huang, S., Liu, X., Wang, D., Chen, W., Hu, Q., Wei, T. et al. (2016) Structural basis for the selective pb(II) recognition of Metalloregulatory protein PbrR691. *Inorganic Chemistry*, 55, 12516–12519.

Hyojin, K., Geupil, J., Bong-Gyu, K. & Youngdae, Y. (2020) Modulation of the metal(loid) specificity of whole-cell bioreporters by genetic engineering of ZntR metal-binding loops. *Journal of Microbiology and Biotechnology*, 30, 681–688.

Ibáñez, M.M., Cerminati, S., Checa, S.K. & Soncini, F.C. (2013) Dissecting the metal selectivity of MerR monovalent metal ion sensors in *Salmonella*. *Journal of Bacteriology*, 195, 3084–3092.

Ibáñez, M.M., Checa, S.K. & Soncini, F.C. (2015) A single serine residue determines selectivity to monovalent metal ions in metalloregulators of the MerR family. *Journal of Bacteriology*, 197, 1606–1613.

Jia, X., Ma, Y., Bu, R., Zhao, T. & Wu, K. (2020) Directed evolution of a transcription factor PbrR to improve lead selectivity and reduce zinc interference through dual selection. *AMB Express*, 10, 67.

Jordan, M.R., Wang, J., Capdevila, D.A. & Giedroc, D.P. (2020) Multimetal nutrient restriction and crosstalk in metallostasis systems in microbial pathogens. *Current Opinion in Microbiology*, 55, 17–25.

Kang, Y., Lee, W., Jang, G., Kim, B.-G. & Yoon, Y. (2018) Modulating the sensing properties of *Escherichia coli*-based bioreporters for cadmium and mercury. *Applied Microbiology and Biotechnology*, 102, 4863–4872.

Khan, S., Brocklehurst, K.R., Jones, G.W. & Morby, A.P. (2002) The functional analysis of directed amino-acid alterations in ZntR from *Escherichia coli*. *Biochemical and Biophysical Research Communications*, 299, 438–445.

Kim, H.J., Jeong, H. & Lee, S.J. (2018) Synthetic biology for microbial heavy metal biosensors. *Analytical and Bioanalytical Chemistry*, 410, 1191–1203.

Kumar, S., Prasad, S., Yadav, K.K., Shrivastava, M., Gupta, N., Nagar, S. et al. (2019) Hazardous heavy metals contamination of vegetables and food chain: role of sustainable remediation approaches - a review. *Environmental Research*, 179, 108792.

Liu, X., Hu, Q., Yang, J., Huang, S., Wei, T., Chen, W. et al. (2019) Selective cadmium regulation mediated by a cooperative binding mechanism in CadR. *Proceedings of the National Academy of Sciences of the United States of America*, 116, 20398–20403.

Martell, D.J., Joshi, C.P., Gaballa, A., Santiago, A.G., Chen, T.-Y., Jung, W. et al. (2015) Metalloregulator CueR biases RNA polymerase's kinetic sampling of dead-end or open complex to repress or activate transcription. *Proceedings of the National Academy of Sciences*, 112, 13467–13472.

Mendoza, J.I., Soncini, F.C. & Checa, S.K. (2020) Engineering of a au-sensor to develop a hg-specific, sensitive and robust whole-cell biosensor for on-site water monitoring. *Chemical Communications*, 56, 6590–6593.

Pérez Audero, M.E., Podoroska, B.M., Ibáñez, M.M., Cauerhff, A., Checa, S.K. & Soncini, F.C. (2010) Target transcription binding sites differentiate two groups of MerR-monovalent metal ion sensors. *Molecular Microbiology*, 78, 853–865.

Pettersen, E.F., Goddard, T.D., Huang, C.C., Couch, G.S., Greenblatt, D.M., Meng, E.C. et al. (2004) UCSF chimera—a visualization system for exploratory research and analysis. *Journal of Computational Chemistry*, 25, 1605–1612.

Philips, S.J., Canalizo-Hernandez, M., Yildirim, I., Schatz, G.C., Mondragón, A. & O'Halloran, T.V. (2015) Allosteric transcriptional regulation via changes in the overall topology of the core promoter. *Science*, 349, 877–881.

Pontel, L.B., Checa, S.K. & Soncini, F.C. (2015) Bacterial copper resistance and virulence. In: Saffarini, D. (Ed.) *Bacteria-metal interactions*. Switzerland: Springer International Publishing, pp. 1–19.

Quintana, J., Novoa-Aponte, L. & Arguello, J.M. (2017) Copper homeostasis networks in the bacterium *Pseudomonas aeruginosa*. *The Journal of Biological Chemistry*, 292, 15691–15704.

Reyes-Caballero, H., Campanello, G.C. & Giedroc, D.P. (2011) Metalloregulatory proteins: metal selectivity and allosteric switching. *Biophysical Chemistry*, 156, 103–114.

Roggo, C. & van der Meer, J.R. (2017) Miniaturized and integrated whole cell living bacterial sensors in field applicable autonomous devices. *Current Opinion in Biotechnology*, 45, 24–33.

Saltepe, B., Kehribar, E.Ş., Su Yirmibeşoğlu, S.S. & Şafak Şeker, U.Ö. (2018) Cellular biosensors with engineered genetic circuits. *ACS Sensors*, 3, 13–26.

Sameach, H., Ghosh, S., Gevorkyan-Airapetov, L., Saxena, S. & Ruthstein, S. (2019) EPR spectroscopy detects various active state conformations of the transcriptional regulator CueR. *Angewandte Chemie International Edition*, 58, 3053–3056.

Sheldon, J.R. & Skaar, E.P. (2019) Metals as phagocyte antimicrobial effectors. *Current Opinion in Immunology*, 60, 1–9.

Szunyogh, D., Szokolai, H., Thulstrup, P.W., Larsen, F.H., Gyurcsik, B., Christensen, N.J. et al. (2015) Specificity of the metalloregulator CueR for monovalent metal ions: possible functional role of a coordinated thiol? *Angewandte Chemie International Edition*, 54, 15756–15761.

Wang, D., Huang, S., Liu, P., Liu, X., He, Y., Chen, W. et al. (2016) Structural analysis of the hg(II)-regulatory protein Tn501 MerR from *Pseudomonas aeruginosa*. *Scientific Reports*, 6, 33391.

Waterhouse, A., Bertoni, M., Bienert, S., Studer, G., Tauriello, G., Gumienny, R. et al. (2018) SWISS-MODEL: homology modelling of protein structures and complexes. *Nucleic Acids Research*, 46, W296–W303.

Xiao, Z., Brose, J., Schimo, S., Ackland, S.M., La Fontaine, S. & Wedd, A.G. (2011) Unification of the copper(I) binding affinities of the Metallo-chaperones Atx1, Atox1, and related proteins: detection probes and affinity standars. *Journal of Biological Chemistry*, 286, 11047–11055.

Zheng, H., Cooper, D.R., Porebski, P.J., Shabalin, I.G., Handing, K.B. & Minor, W. (2017) CheckMyMetal: a macromolecular metal-binding validation tool. *Acta Crystallographica Section D*, 73, 223–233.

SUPPORTING INFORMATION

Additional supporting information can be found online in the Supporting Information section at the end of this article.

How to cite this article: Mendoza, J.I., Lescano, J., Soncini, F.C. & Checa, S.K. (2022) The protein scaffold calibrates metal specificity and activation in MerR sensors. *Microbial Biotechnology*, 15, 2992–3002. Available from: https://doi.org/10.1111/1751-7915.14151